

## Near-field light concentration of ultra-small metallic nanoparticles for absorption enhancement in a-Si solar cells

Boyuan Cai,<sup>1</sup> Baohua Jia,<sup>1,a)</sup> Zhengrong Shi,<sup>2</sup> and Min Gu<sup>1,a)</sup>

<sup>1</sup>Centre for Micro-Photonics, Faculty of Engineering and Industrial Sciences, Swinburne University of Technology, PO Box 218, Hawthorn, 3122 Victoria, Australia

<sup>2</sup>Suntech Power Holdings Co., Ltd., 9 Xinhua Road, New District, Wuxi, Jiangsu Province 214028, China

(Received 29 November 2012; accepted 21 February 2013; published online 5 March 2013)

Near-field light concentration from plasmonic nanostructures was predicted to significantly improve solar cell conversion efficiency since the inception of plasmonic solar cells. However the challenge remains in designing effective nanostructures for useful near-field enhancement much exceeding the detrimental ohmic loss and light blockage losses in solar cells. We propose and demonstrate ultra-small (a few nanometers) gold nanoparticles integrated in amorphous silicon solar cells between the front electrode and the photoactive layer. Significant enhancements in both the photocurrent (14.1%) and fill factor (12.3%) have been achieved due to the strong plasmonic near-field concentration and the reduced contact resistance, respectively. © 2013 American Institute of Physics.

[<http://dx.doi.org/10.1063/1.4794420>]

Plasmonic nanoparticles have been proved to be highly effective in improving the performance of diverse solar cells, including organic solar cells,<sup>1,2</sup> dye sensitized solar cells,<sup>3</sup> crystalline silicon solar cells,<sup>4–6</sup> and silicon thin-film solar cells.<sup>7–9</sup> The reported enhancement mechanism is mainly the photocurrent improvement induced by the plasmonic resonant scattering associated with comparatively large nanoparticles ( $\sim 100$  nm).<sup>10</sup> Although the plasmonic near-field light concentration has been theoretically predicted to be able to dramatically increase the charge-carrier generation in solar cells,<sup>11–15</sup> experimental demonstration is greatly limited.<sup>1</sup> The challenges mainly lie in two aspects. First, the near-field light concentration is always accompanied by strong ohmic loss from the nanoparticles, which is dissipated as heat. To solve this problem the nanoparticles need to be designed to possess the highest localized field enhancement much exceeding the absorption loss from the particles themselves. Second, to fully utilize the large field concentration, the nanoparticles should be placed in the close vicinity of the photoactive layer, where the electron-hole pairs are generated. This often means that the nanoparticles need to be on the front surface or embedded in the active layer of the solar cells, which could lead to severe light blockage loss.

In this paper, we propose to harness the plasmonic near-field light concentration in amorphous silicon (a-Si) solar cells by using ultra-small gold nanoparticles of a few nanometers placed on the front side of the solar cells between the textured transparent conductive oxide (TCO) glass and the silicon layer. Because of the ultra-high localization, the nanoparticles possess strong field enhancement much exceeding the particle absorption loss. In the meantime the small particle size and the low surface coverage do not cause a significant light blockage loss even when the particles are on the front side of the solar cell close to the active layer.

Consequently, broadband (from 350 to 800 nm) solar cell absorption enhancement is demonstrated, which is a

challenge to achieve with rear located particles because light at the shorter wavelength region cannot penetrate the solar cell and reach the nanoparticles effectively.<sup>9,16,17</sup> At optimized particle size and surface coverage (SC), a maximum short circuit current ( $J_{sc}$ ) enhancement of 14.1% is achieved. In addition to the photocurrent enhancement, the fill factor (FF) of the optimized cell is increased by 12.3% contributing to the final efficiency improvement of 33%.

The ultra-small gold nanoparticles were made by the simple thermal evaporation method. To control the particle size to be a few nanometers, gold films with sub-nanometer to a few nanometer thicknesses need to be deposited first. By carefully controlling the deposition speed, ultra-small nanoparticles with different sizes and SCs can be formed. In our experiment we deposited five different thicknesses, which are 0.3 nm, 0.6 nm, 0.8 nm, 1 nm, and 1.8 nm, respectively. Figs. 1(a)–1(c) show the SEM images of selected Au nanoparticles uniformly deposited on the surface of the ZnO:Al layer which is coated on glass. It can be observed that the sizes and SCs of the nanoparticles increase with increased film thickness. The mean sizes are approximately 7 nm ( $\pm 2$  nm) with 27% SC, 10 nm ( $\pm 2.5$  nm) with 49.7% SC, and 14 nm ( $\pm 3$  nm) with 84.2% SC for films with 0.6 nm, 1.0 nm, and 1.8 nm thicknesses, respectively.

The transmittance curves of the ZnO:Al glass integrated with gold nanoparticles of five different sizes measured with a spectrometer (Perkin Elmer, Lambda 1050) are shown in Fig. 1(d). From the transmittance curves, we can see that the localized surface plasmonic resonance (LSPR) peaks (corresponding to the dip in the transmittance) of Au nanoparticles redshift from 550 nm to 650 nm with increased thicknesses from 0.6 nm to 1.8 nm mainly because of the increase in particles size. For larger particle size and higher SCs of Au nanoparticles, the particle absorption becomes so strong that the light transmittance is reduced.

To examine the influence of the ultra-small nanoparticles on the solar cells, a-Si layers with an overall thickness of 260 nm were deposited by the plasma enhanced chemical vapor deposition (PECVD) method on top of the nanoparticle

<sup>a)</sup> Authors to whom correspondence should be addressed. Electronic addresses: [bjia@swin.edu.au](mailto:bjia@swin.edu.au) and [mgu@swin.edu.au](mailto:mgu@swin.edu.au).

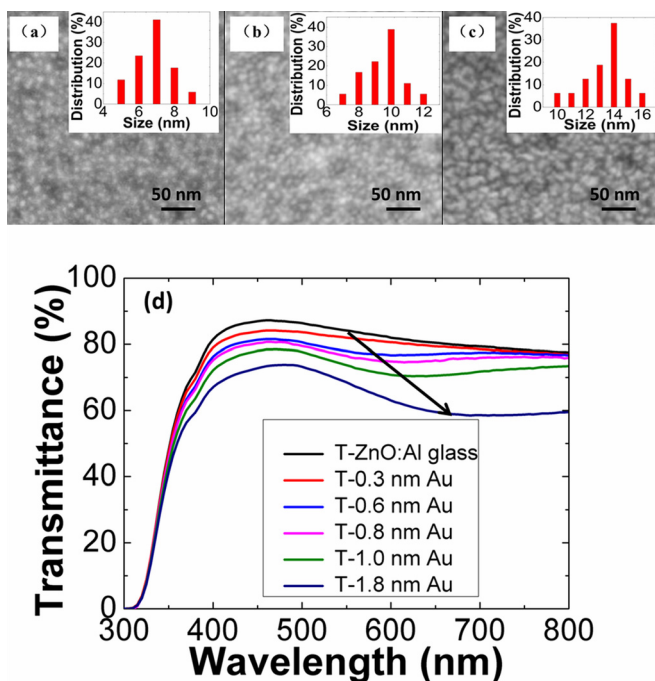


FIG. 1. SEM images of different sizes of Au nanoparticles (a)  $\sim 7$  nm ( $\pm 2$  nm), (b)  $\sim 10$  nm ( $\pm 2.5$  nm), (c)  $\sim 14$  nm ( $\pm 3$  nm) on the surface of ZnO:Al layers corresponding to film thicknesses of 0.6 nm, 1 nm, and 1.8 nm, respectively. (d) Transmittance of ZnO:Al glass with an Au layer of 0.3 nm, 0.6 nm, 0.8 nm, 1 nm, 1.8 nm in thickness.

integrated TCO glass as shown in Fig. 2. At last a ZnO:Al layer with 100nm in thickness and an Ag back reflector layer with 180nm in thickness was deposited. The standard current density-voltage ( $I$ - $V$ , Oriol Sol 3ATM class AAA, model 94023 A) and external quantum efficiency (EQE, PV Measurements, Inc., Model QEX10) measurements were used to characterize the solar cells.

It is clearly shown in Fig. 1(d) that as the size and SC of the nanoparticles become too large, the particle absorption loss becomes non-ignorable, which leads to reduced photocurrent generation. However,  $FF$  is expected to increase due to the reduced contact resistance between the TCO glass and the a-Si layer. Therefore, there exists an optimized condition for the best values of  $J_{sc}$  and  $FF$ . To find this condition, we plot the normalized values of  $J_{sc}$  and  $FF$ , the open circuit voltage ( $V_{oc}$ ), and efficiency of the solar cells integrated with ultra-small Au nanoparticles to the reference cells as a function of the film thickness as shown in Fig. 3.

It can be seen from Fig. 3(a) that the  $FF$  enhancement increases steadily with increased Au film thickness as expected. In the meantime  $J_{sc}$  and  $V_{oc}$  enhancement decreases with increased Au film thickness except for the thicknesses of 0.5 nm and 0.6 nm. For a 0.3 nm Au film an

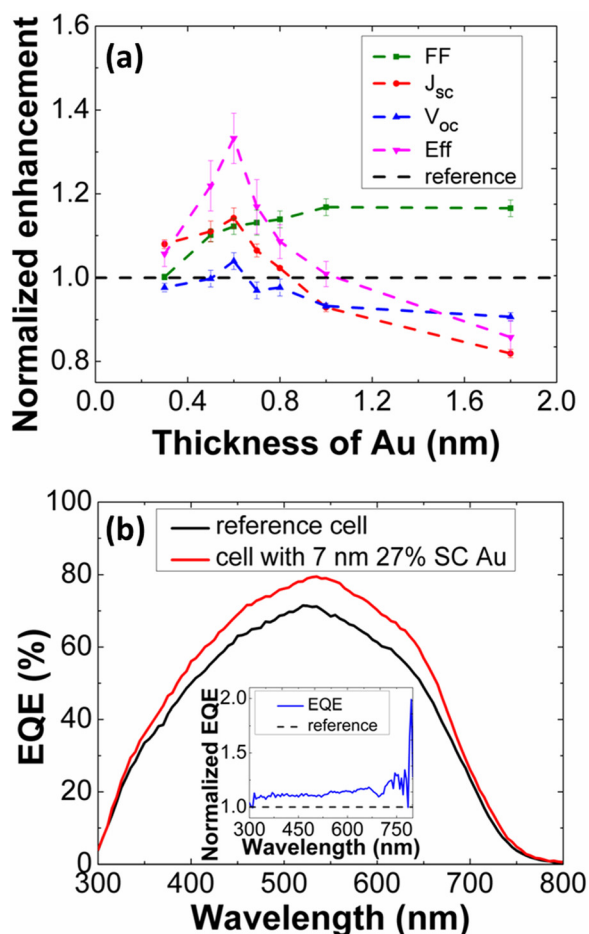


FIG. 3. (a) Normalized enhancements of a-Si solar cell parameters with different thicknesses of Au nanoparticles. (b) EQE for solar cells with/without Au nanoparticles.

enhancement of 7% in  $J_{sc}$  is observed. When the thickness of the Au film increases to 0.6 nm, a peak enhancement in  $J_{sc}$  of 14.1% is achieved. When the thickness is further increased, both the SC and the particle size become larger, which leads to the increased particle absorption loss outweighing the plasmonic near-field enhancement. Therefore  $J_{sc}$  starts to reduce. So there is a competing process between the plasmonic near-field enhancement, which leads to the solar cell absorption enhancement, and the absorption loss by the Au nanoparticles, which reduces the light absorption by the a-Si solar cells.

From Fig. 3(a), we can easily identify that the optimized film thickness to achieve the best solar cell efficiency enhancement is 0.6 nm. Under such a circumstance,  $J_{sc}$  is improved from 12.4 mA/cm<sup>2</sup> to 14.15 mA/cm<sup>2</sup>, while  $FF$  is improved from 34.88% to 39.16%. The Au nanoparticles effectively lower to the Shorttky barrier height and provide a better ohmic

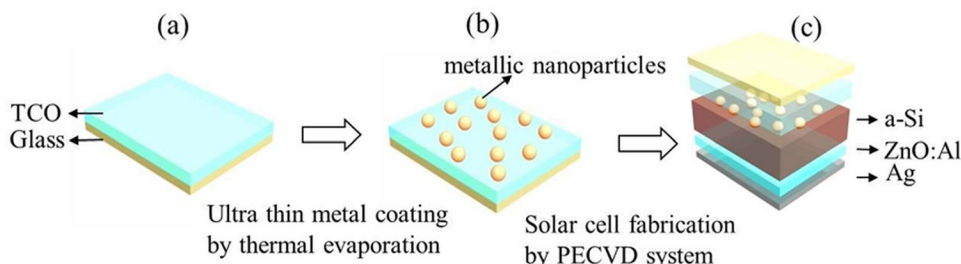


FIG. 2. The sketch of the a-Si solar cell with Au nanoparticles.

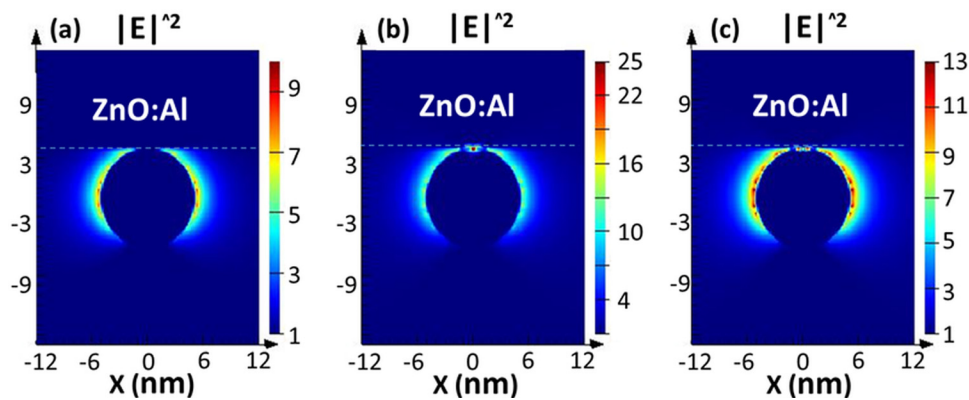


FIG. 4. The light intensity around 10 nm Au nanoparticles on ZnO:Al substrate at different wavelengths: (a) 400 nm, (b) 580 nm, (c) 650 nm.

contact to the a-Si than the TCO electrode.<sup>18</sup> The measured series resistance of the optimized solar cell with Au nanoparticles is  $12.8 \Omega$  compared with  $17.1 \Omega$  without the Au nanoparticles. To further analyze the mechanism of the enhancement, we measured the spectral response (EQE) of the solar cell with the best enhancement, as shown in Fig. 3(b).

For a-Si solar cells, the largest value of EQE is around 550 nm, which is in accordance with the resonance peak of the Au nanoparticles shown in Fig. 1(b). From the SEM image in Fig. 1(a), the sizes of the 0.6 nm thick Au nanoparticles are less than 10 nm in diameter. So the plasmonic scattering effect can be ignored under such a situation. We believe the increase in  $J_{sc}$  is mainly owing to the plasmonic near-field enhancement of the Au nanoparticles, which makes more light absorbed by the photoactive layer. The light is strongly concentrated due to the localized surface plasmon resonance of Au nanoparticles, which increases the light absorption of the a-Si near the Au nanoparticles. In addition, the carrier mobility is increased due to the more conductive metallic nanoparticles than the TCO materials,<sup>19</sup> which may also lead to a broadband enhancement in the EQE curve.

To further confirm that the origin of the enhancement is due to the plasmonic near-field concentration, we calculated the near-field light intensity distributions of a 10 nm Au nanoparticle on the ZnO:Al substrate, which mimic the same condition on experiment, under different wavelength light illumination as shown in Fig. 4. In our simulation, the light incident direction is  $-Z$ . It can be seen that the light intensity around the Au nanoparticles is enhanced as high as 25 folds at 580 nm wavelength, red-shifting from 530 nm in vacuum to 580 nm when Au particle is placed on the ZnO:Al substrate. The near field enhancement is around 10 folds at other wavelengths.

In summary, we have demonstrated that tailored ultra-small gold nanoparticles on the front side of solar cells are a simple solution that can effectively harness strong near-field enhancement leading to significant performance improvement of a-Si solar cells. Both the short circuit current and the fill factor can be optimized. These findings offer a new approach to achieve a plasmonic near-field enhancement.

The authors acknowledge the access to the Victoria-Suntech Advanced Solar Facility (VSASF) established under and Victoria Science Agenda (VSA) scheme by the Victorian Government. Boyuan Cai thanks Suntech Power Holdings Co. Pty. for his Ph.D. scholarship. B.J. thanks L'Oréal for providing support through the L'Oréal Australia and New Zealand for Women in Science Fellowship.

- <sup>1</sup>J. Yang, J. You, C. C. Chen, W. C. Hsu, H. R. Tan, X. W. Zhang, Z. Hong, and Y. Yang, *ACS Nano* **5**, 6210 (2011).
- <sup>2</sup>Y. Hsiao, S. Charan, F. Wu, F. Chien, C. Chu, P. Chen, and F. Chen, *J. Phys. Chem. C* **116**, 20731 (2012).
- <sup>3</sup>C. Hägglund, M. Zäch, and B. Kasemo, *Appl. Phys. Lett.* **92**, 013113 (2008).
- <sup>4</sup>S. Pillai, K. R. Catchpole, T. Trupke, and M. A. Green, *J. Appl. Phys.* **101**, 093105 (2007).
- <sup>5</sup>N. Fahim, Z. Ouyang, Y. Zhang, B. Jia, Z. Shi, and M. Gu, *Opt. Mater. Express* **2**, 190 (2012).
- <sup>6</sup>Y. Zhang, Z. Ouyang, N. Stokes, B. Jia, Z. Shi, and M. Gu, *Appl. Phys. Lett.* **100**, 151101 (2012).
- <sup>7</sup>D. Derkacs, S. H. Lim, P. Matheu, W. Mar, and E. T. Yuerkacs, *Appl. Phys. Lett.* **89**, 093103 (2006).
- <sup>8</sup>V. E. Ferry, M. A. Verschuuren, H. B. T. Li, E. Verhagen, R. J. Walters, R. E. I. Schropp, H. A. Atwater, and A. Polman, *Opt. Express* **18**, A237 (2010).
- <sup>9</sup>X. Chen, B. Jia, J. K. Saha, B. Cai, N. Stokes, Q. Qiao, Y. Wang, Z. Shi, and M. Gu, *Nano Lett.* **12**, 2187 (2012).
- <sup>10</sup>M. Gu, Z. Ouyang, B. Jia, N. Stokes, X. Chen, N. Fahim, X. Li, M. J. Ventura, and Z. Shi, *Nanophotonics* **1**, 1 (2012).
- <sup>11</sup>M. J. Mendes, A. Luque, I. Tobias, and A. Marti, *Appl. Phys. Lett.* **95**, 071105 (2009).
- <sup>12</sup>N. Lagos, M. M. Sigalas, and E. Lidorikis, *Appl. Phys. Lett.* **99**, 063304 (2011).
- <sup>13</sup>H. A. Atwater and A. Polman, *Nat. Mater.* **9**, 205 (2010).
- <sup>14</sup>C. Hägglund and S. P. Apell, *J. Phys. Chem. Lett.* **3**, 1275 (2012).
- <sup>15</sup>P. Spinelli and A. Polman, *Opt. Express* **20**, A641 (2012).
- <sup>16</sup>C. Eminian, F.-J. Haug, O. Cubero, X. Niquille, and C. Ballif, *Prog. Photovoltaics* **19**, 260 (2011).
- <sup>17</sup>H. Tan, R. Santbergen, A. H. M. Smets, and M. Zeman, *Nano Lett.* **12**, 4070 (2012).
- <sup>18</sup>T. Markvart and L. Castner, *Practical Handbook of Photovoltaics Fundamentals and Applications. Part II C* (Elsevier, 2003).
- <sup>19</sup>M. Xue, L. Li, B. J. Tremolet de Villers, H. Shen, J. Zhu, Z. Yu, A. Z. Stieg, Q. Pei, B. J. Schwartz, and K. L. Wang, *Appl. Phys. Lett.* **98**, 253302 (2011).